A Theoretical Study of Circular Orthotropic Membrane Under Concentrated Load: The Relation of Load and Deflection

PENGFEI HUANG[ID][1], YANPING SONG[1], QI LI[2], XIAOQI LIU[1], AND YUQING FENG[1]
[1]China Academy of Space Technology (Xi'an), Xi'an 710100, China
[2]Northwestern Polytechnical University, Xi'an 710072, China

Corresponding author: Pengfei Huang (pengf_huang@outlook.com)

ABSTRACT In this study, the deformation of circular orthotropic membranes subjected to a central concentrated force is investigated. An orthotropic membrane equation indicating load-deflection behavior based on Föppl-von Kármán membrane theory is obtained and the numerical solutions are gotten by using MATLAB. A variable k, which is the most influential parameter on the load-deflection behavior, is proposed. In isotropic membrane, the change of material parameters mainly influences the deflection of membranes subjected to a concentrated force; however, when studying for orthotropic membrane, the shape of membrane after deformation can be controlled by changing the value of k. Only change in elastic modulus and Poisson's ratio, with k constant, mainly influence the deflection of curves, instead of the shape of curves. Then, four numerical simulations by ABAQUS are conducted and the membrane element M3D4R is used to set up a finite-element model. By comparing these simulation results with the solutions from orthotropic membrane equation, it is shown that the orthotropic membrane equation gives a good estimation of load-deflection behavior.

INDEX TERMS Load-deflection curve, orthotropic membrane, central concentrated load, membrane element M3D4R.

I. INTRODUCTION

Recent interest in membrane structures has created numerous and unique challenges related to many advanced technologies [1]–[3], such as micro-electro-mechanical systems (MEMS) and space shuttle. Space mesh reflector (SMR) antennas are irreplaceable in the field of aerospace because of its lightweight, high packaging efficiency, and potential to realize large-scale extension and high surface accuracy [4]. Existing large SMR uses metal meshes as a reflecting surface. The reflectors are often analyzed as membrane due to its low compressive and bending stiffness [4], [5]. When working in orbit, the antenna reflector needs to keep an exact paraboloidal shape, which is directly determined by the tension on the metal meshes [6]. Therefore, in order to maintain high surface accuracy, the problem of the large deformation of a circular membrane under a concentrated force is of great significance. Fig. 1 shows the schematic the problem. The research on the membrane structures commenced with the
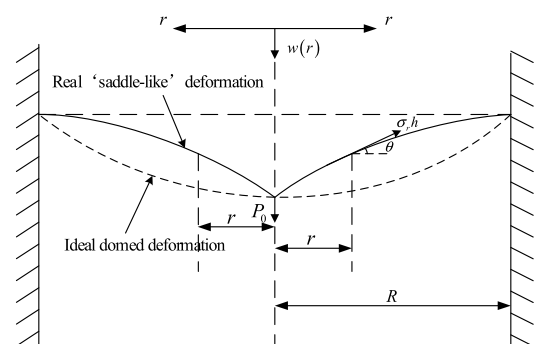

**FIGURE 1.** Schematic of membrane subjected a central concentrated load.

work of Henchy [7], who gave the solution to the large deflection of the clamped circular membrane under uniform load in 1915. Then Chien [8] and Alekseev [9] had some modifications on Henchy's solution. With the use of an intermediate parameter and a controlled parameter, an exact analytical solution of the quantitative relation (load vs. deflection) of the membrane under centrally concentrated load was proposed [10]. The solutions could be used for the measurement

of mechanical properties of ultra-thin membrane neglecting the flexural rigidity. Besides, extensive research has been conducted on other related membrane problems. Wan [11] derived analytical constitutive relations based on an average membrane stress approximation and compared the results with finite-element analysis. It should be pointed out that they did not confine the thickness and flexural rigidity of the film to a small range but spanned a wide spectrum. An experimental study, along with theoretical analysis, was presented by Ju [12] for characterizing the mechanical properties and adhesion of a thin polymer membrane, primarily Young's modules. Lim [13] explored the deflection of circular membranes when the membrane material is auxetic and considered that auxetic membranes exhibited greater flexibility and stretching (bio) functions in comparison with conventional membranes, at equal Young's modulus. Jensen [14] studied the effect of Poisson's ratio on material deformation; while, the influence of parameters including sample thickness, indentation depth and indenter size was also analyzed.

The above solutions for circular thin membrane problems are all in the linear elastic domains and the constitutive equations are mainly based on Föppl–von Kármán membrane theory. When the deformation and the size of membrane are of the same order, the solution of the large deformation mentioned above cannot meet the requirements. Therefore, recent developments in the theory of non-linear elasticity were given in the noteworthy survey volume by Fu and Ogden [15]. Besides, A.P.S. Selvadurai [16] concluded four different hyper-elastic constitutive models and got the deflection of rubber membrane based on these models. His results agreed well with experimental study. The governing equations of large deformations of 3D hyperelastic solids are derived by the minimum total potential energy principle, and the Neo-Hookean model is used for the hyperelastic character of material [17]. The hybrid nanocomposite plate deformation is formulated based on classical plate theory and the contact force between the plate and projectile is estimated using Hertzian contact law [18]. Pugno [19] developed a theoretical-numerical approach to simulate the detachment of an elastic membrane of finite size from a substrate, using a 3D cohesive law. It was of great success and significance because the model was validated by analytical results for simple geometries, and has also been applied in a series of parametric studies. Their methods can be useful to model a membrane structures when we take non-linear elasticity into account. Besides, many scholars studied the vibration control of membrane. A plate membrane model and a pure membrane model have been studied respectively to achieve active vibration control of plate membrane mirrors [20]. A closed-loop membrane mirror shape control system is set up and a surface shape control method based on an influence function matrix of the mirror is then investigated [21]. To analyze the nonlinear dynamic characteristics of the membrane, the theoretical and approximate solutions of nonlinear frequencies of the membrane are obtained, and the discrepancies between

the two solutions under different vibration amplitudes are discussed [22].

The references mentioned above mainly studied the isotropic membrane. As for the orthotropic membrane, much work had also been completed. The stochastic dynamic response and reliability analysis of membrane structure under impact load obeying Gaussian distribution was investigated by Li [23]. Banichuk [24] derived the analytical solution originally to develop for isotropic axially moving plates and then extended it to general orthotropic case. Jesús [25] presented a formulation for the geometrically nonlinear analysis of orthotropic membrane structures and an algorithm for modeling the wrinkling behavior of membrane structures.
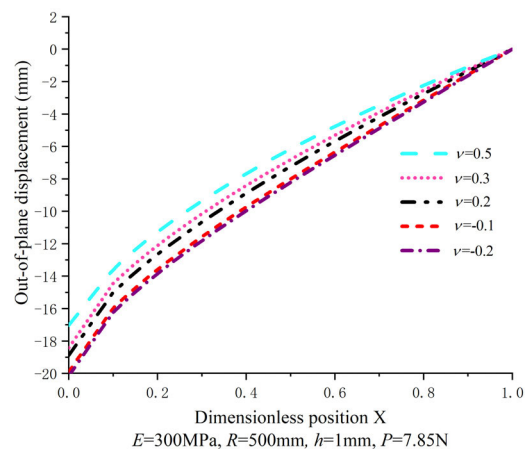
FIGURE 2. Effect of Poisson's ratio on load-deflection behavior for circular isotropic membrane.

According to the summary of literature above, the results show that isotropic circular membrane always presented a 'saddle-like' deformation after subjected to a concentrated force (see Fig. 1); meanwhile, the results from the solutions of Sun [10] revealed that changes in Poisson's ratio of membrane only influences the curves' deflection, but not its shape as is shown in Fig. 2. Because the circular membrane is centrosymmetric, for simplification, for simplification, all the load-deflection curves in this paper only presents half the membrane. However, an ideal domed deformation shown in Fig. 1, which can [26] overcome some problems such as aircraft wings, car doors, is desired and it can also help simplify many other engineering structures. Unfortunately, the work which focused on orthotropic membrane almost not studied the load-deflection behavior subjected to such a central load as shown Fig. 1. Therefore, motivated by the preceding analyses, this kind of static problem on orthotropic membrane are studied in this paper.

A new analytical method is proposed for determining the deflection of orthotropic membrane subjected to a concentrated force in the center of the membrane. Based on the work of Sun [10], we have obtained the orthotropic membrane equation and gotten the numerical solution using MATLAB.
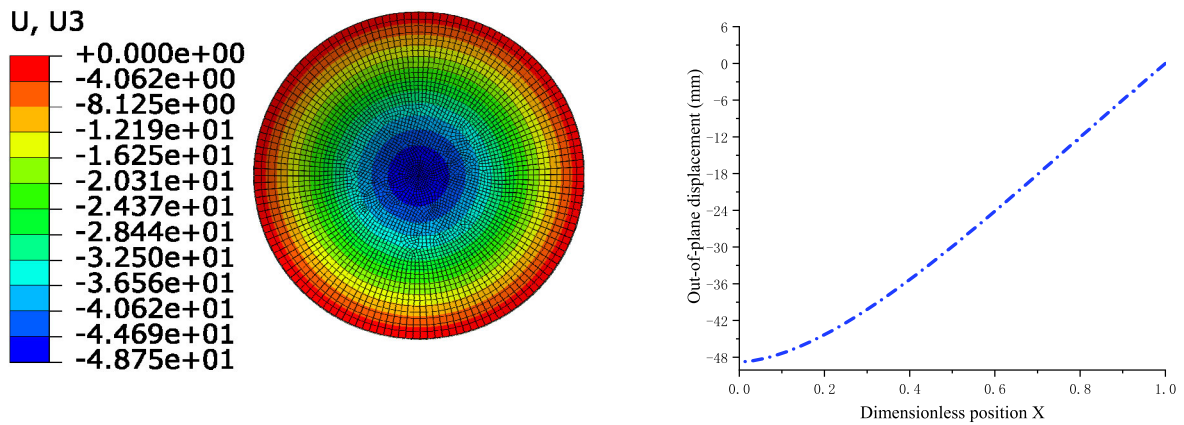
FIGURE 3. Deformation of model using shell element subjected a central concentrated load.
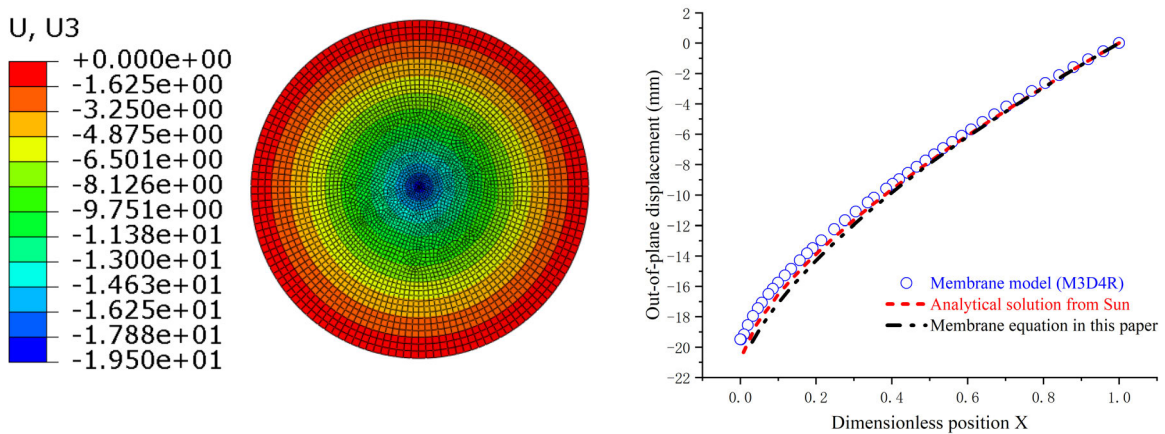

FIGURE 4. Comparison of load-deflection curves between analytical solution and ABAQUS model.

TABLE 1. The parameters during calculations with the change of k.

k	$F(N)$	v_r	v_t	$E_r(MPa)$	$E_t(MPa)$	$Z\big|_{x=0}$	$dZ/dx\big|_{x=0}$	Δ
1	0.7854	0.3	0.3	300	300	0.1857843	120.7597	7.7e-5
0.67	0.7854	0.3	0.2	300	200	0.3031856	181.9113	1.1e-4
0.33	0.7854	0.3	0.1	300	100	0.7094480	390.1964	1.7e-5
0.03	0.7854	0.3	0.01	300	10	10.129830	5115.564	5.3e-5
0.0003	0.7854	0.3	0.0001	300	0.1	1123.8060	561959.2	1.3e-5

A variable k, which is the most influential parameter on the load-deflection behavior, is proposed. The value of k combines the action of Poisson's ration and elastic modulus. When studying orthotropic membrane, the deformation of membrane can be controlled by adjusting the value of k. Besides, some numerical simulations by ABAQUS are conducted using membrane element M3D4R, which are compared with the solution of orthotropic membrane equation.

This paper is structured as follows. In section 2, the orthotropic membrane equation is obtained. In section 3, a membrane model is set up within the platform ABAQUS
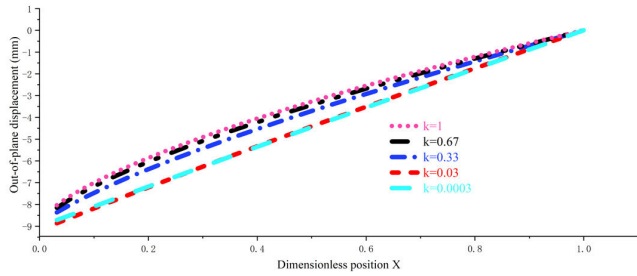
FIGURE 5. Effect of k on load-deflection behavior for circular orthotropic membrane.

applying the membrane element M3D4R. In section 4, several numerical examples are performed and the effect of model parameters on load-deflection curves is discussed.

II. THE ORTHOTROPIC MEMBRANE EQUATION AND ITS SOLUTION

Suppose we take a piece of the circular membrane of radius r with $r \leq R$, as shown in Fig. 1.
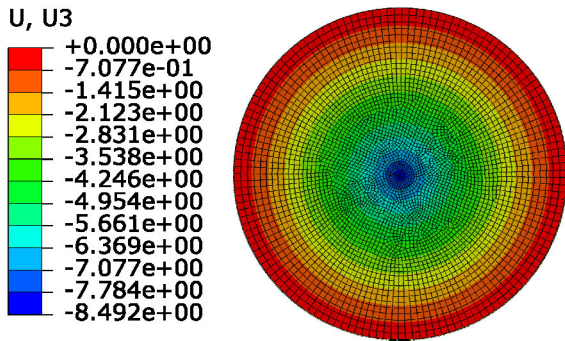
The paper studies the static problem of equilibrium of a membrane under concentrated force P_0 and membrane force $\sigma_r h$ acted on the boundary. We assume that the membranes were sufficiently thin to neglect the normal stress and transverse shear strain. In addition, when undertaking the external normal load, the bending moment is not under consideration. Therefore, there are two vertical forces, the P_0 and the total vertical force $2\pi r h \sigma_r \sin \theta$, which is produced by the membrane force $\sigma_r h$, in which h is the thickness of the membrane, and θ is the angle.

As shown in Fig. 1, considering the equilibrium of vertical force and equilibrium condition in the plane of the membrane [10], we have the following equations.

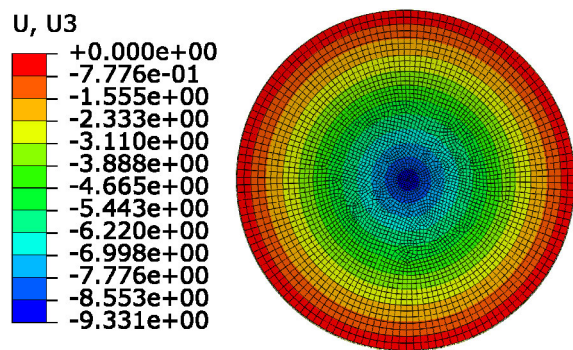$$2\pi r h \sigma_r \frac{dw}{dr} = -P_0 \tag{1}$$

$$\frac{d}{dr}(rh\sigma_r) - h\sigma_t = 0 \tag{2}$$

$$\left.\begin{array}{l} \varepsilon_r = \dfrac{du}{dr} + \dfrac{1}{2}\left(\dfrac{dw}{dr}\right)^2 \\ \\ \varepsilon_t = \dfrac{u}{r} \end{array}\right\} \tag{3}$$
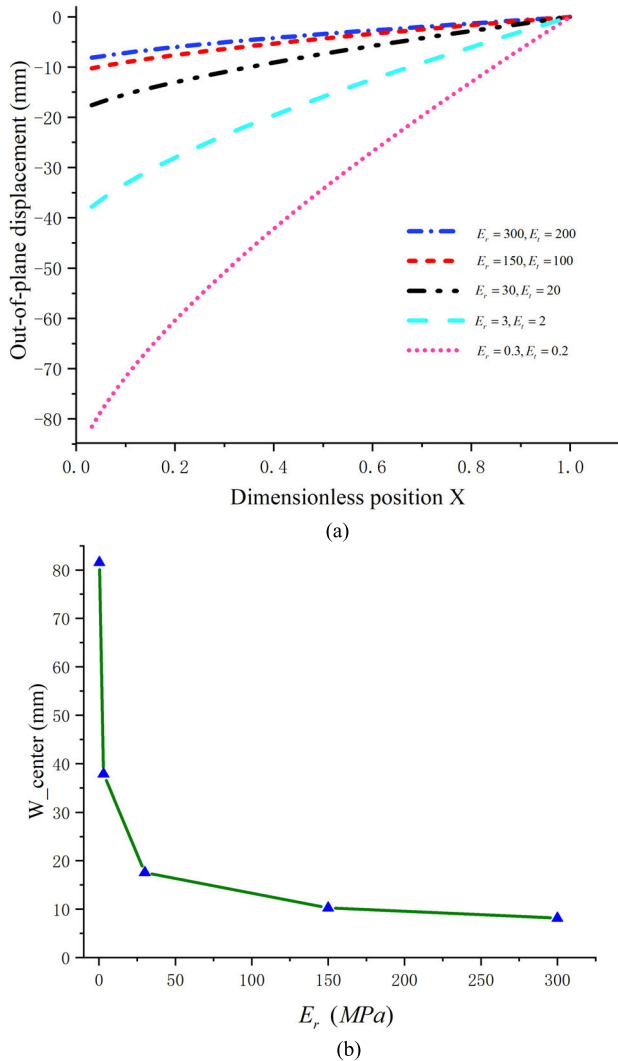

(a) k=0.67

(b) k=0.03

FIGURE 6. Comparison of load-deflection curves resulted from membrane equations and ABAQUS model.

FIGURE 7. (a) Effect of elastic modulus on load-deflection behavior. (b) Effect of elastic modulus on the deflection of central point.

where $\sigma_r h$ is the radial membrane force, $\sigma_t h$ is the circumferential membrane force, ε_r is the radial strain, ε_t is the circumferential strain, $u(r)$ is the radial displacement and $w(r)$ is the transversal displacement.

The relation between the stress and the strain of orthotropic membrane are

$$\left.\begin{aligned}
\sigma_r &= \frac{E_r}{1 - \nu_t \nu_r}(\varepsilon_r + \nu_t \varepsilon_t) \\
\sigma_t &= \frac{E_t}{1 - \nu_t \nu_r}(\varepsilon_t + \nu_r \varepsilon_r)
\end{aligned}\right\} \quad (4)$$

in which E_r is radial Young's modulus; E_t is circumferential Young's modulus; ν_r is radial Poisson's ratio; ν_t is circumferential Poisson's ratio. Substituting Eq. (3) into Eq. (4), we have

$$\left.\begin{aligned}
h\sigma_r &= \frac{E_r h}{1 - \nu_t \nu_r}\left(\frac{du}{dr} + \frac{1}{2}\left(\frac{dw}{dr}\right)^2 + \nu_t \frac{u}{r}\right) \\
h\sigma_t &= \frac{E_t h}{1 - \nu_t \nu_r}\left[\frac{u}{r} + \nu_r \frac{du}{dr} + \frac{\nu_r}{2}\left(\frac{dw}{dr}\right)^2\right]
\end{aligned}\right\} \quad (5)$$

By combination of Eq. (5) and Eq. (2), we have

$$\frac{u}{r} = \frac{1}{E_t}\frac{d}{dr}(r\sigma_r) - \frac{\nu_r \sigma_r}{E_r} \quad (6)$$

Substitute Eq. (6) into the first expression of Eq. (5), then

$$-\frac{1}{E_t} \cdot r \cdot \frac{d}{dr}\left[\frac{1}{r}\frac{d}{dr}\left(r^2 \sigma_r\right)\right] + \left[\frac{1}{E_r} - \frac{1}{E_t}\right] \cdot \sigma_r = \frac{1}{2}\left(\frac{dw}{dr}\right)^2 \quad (7)$$

Introduce the following variables

$$\left.\begin{aligned}
x &= \frac{r^2}{a^2}, \quad S_{r1} = \frac{a^2}{E_t h^2}\sigma_r \\
S_{r2} &= \frac{a^2}{E_r h^2}\sigma_r
\end{aligned}\right\},$$

$$P = \frac{P_0 a^2}{E_t h^4 \cdot 4\pi}, \quad W = \frac{w}{h} \quad (8)$$

Meanwhile, we get

$$\frac{d}{dr} = \frac{d}{dx} \cdot \frac{dx}{dr} = \frac{2r}{a^2}\frac{d}{dx} \quad (9)$$

Substitute Eq. (8) and Eq. (9) into Eq. (7), we have

$$\frac{d^2(xS_{r1})}{dx^2} \cdot 4x - \left[\frac{xS_{r2}}{x} - \frac{xS_{r1}}{x}\right] + 2x\left(\frac{dW}{dx}\right)^2 = 0 \quad (10)$$

Then

$$\frac{d^2(xS_{r1})}{dx^2} \cdot 4x^2 - [xS_{r2} - xS_{r1}] + 2x^2\left(\frac{dW}{dx}\right)^2 = 0 \quad (11)$$

Substitute Eq. (8) into Eq. (1), we obtain

$$xS_{r1}\frac{dW}{dx} = -P \quad (12)$$

Again, some variables are introduced here

$$\left.\begin{aligned}
xS_{r1} &= Z_1 \\
xS_{r2} &= Z_2
\end{aligned}\right\}, \quad k = \frac{S_{r2}}{S_{r1}} = \frac{E_t}{E_r} = \frac{\nu_t}{\nu_r} \quad (13)$$

Substitute Eq. (13) into Eq. (11), we have

$$\left.\begin{aligned}
\frac{d^2(Z_1)}{dx^2} + \frac{(1-k)}{4x^2}Z_1 + \frac{P^2}{2Z_1^2} &= 0 \\
Z_1\frac{dW}{dx} &= -P
\end{aligned}\right\} \quad (14a, b)$$

Therefore, we get the orthotropic membrane equation Eq. (14) and the boundary condition under which the equations could be solved are

$$\frac{u}{r} = 0 \quad \text{at } x = 0;$$
$$\frac{u}{r} = 0 \quad \text{and } W = 0 \quad \text{at } x = 1; \quad (15a, b, c)$$

Then, by solving Eq. 14(a, b), a sequence of load-deflection curves can be obtained. It is obvious that k is the key factor to the results of the equations. So, we will focus on the effect of k on equations results in following sections. However, for such nonlinear second-order differential equations, it is hard to get their analytical solutions. Therefore, we will try to solve it using ODE45 method in MATLAB in section 4.

TABLE 2. The parameters during calculations with the change of elastic modulus.

k	$F(N)$	v_r	v_t	$E_r(MPa)$	$E_t(MPa)$	$Z\|_{x=0}$	$dZ/dx\|_{x=0}$	Δ
0.67	0.7854	0.3	0.2	300	200	0.3031856	181.9113	1.1e-4
0.67	0.7854	0.3	0.2	150	100	0.481277	288.7662	8.9e-5
0.67	0.7854	0.3	0.2	30	20	1.407262	844.3576	8.0e-5
0.67	0.7854	0.3	0.2	3	2	6.531935	3919.161	7.6e-4
0.67	0.7854	0.3	0.2	0.3	0.2	30.31855	18191.13	1.1e-5

(a) $E_r = 150MPa, E_t = 100MPa$
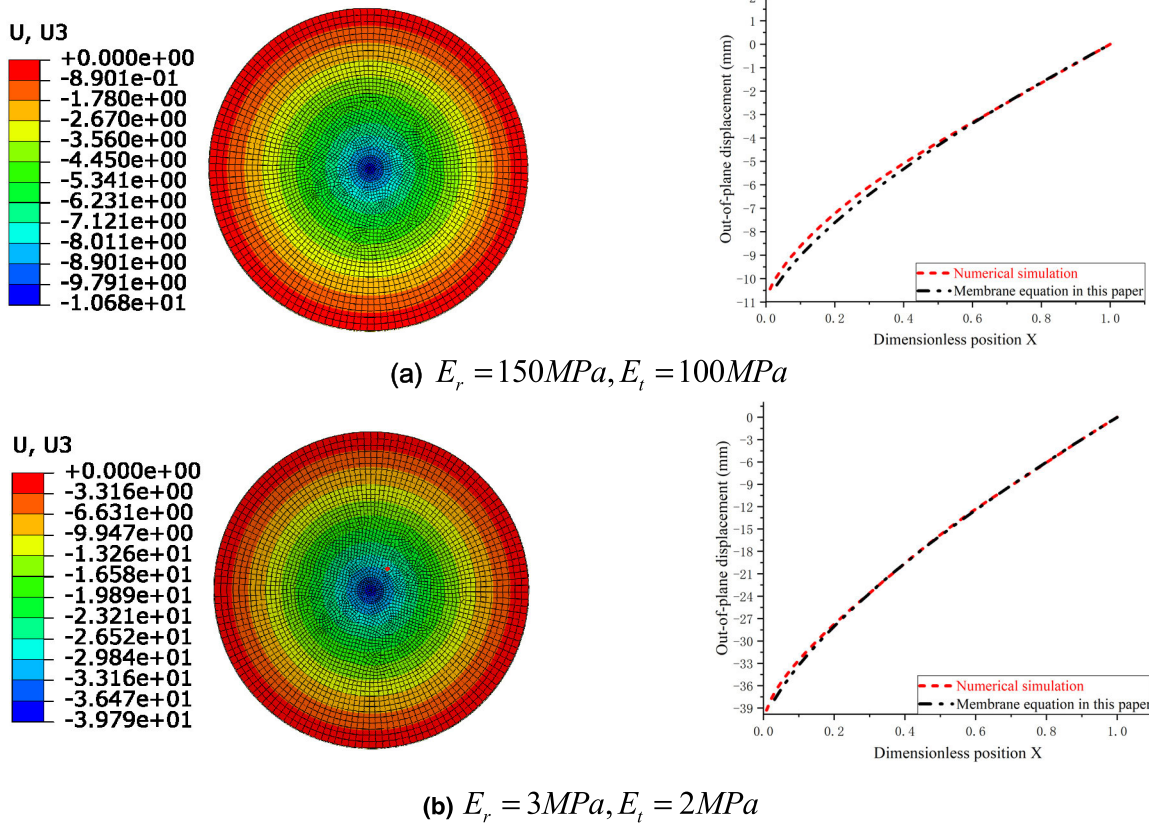
(b) $E_r = 3MPa, E_t = 2MPa$

FIGURE 8. Comparison of load-deflection curves resulted from membrane equations and ABAQUS model.

III. NUMERICAL SIMULATION USING ABAQUS
A. FINITE-ELEMENT MODEL
In sequential analysis, a 3D model of circular membrane is set up in ABAQUS/standard with the geometrical parameters as: $R = 500mm$, $h = 1mm$. When studying membrane, many scholars modeled in ABAQUS using shell element [27], [28], such as S4R, S8R5. However, shell elements (S4R) cannot give a nice simulation to real deformation of circular membrane subjected to a load at central point shown as Fig. 3. Therefore, membrane element M3D4R (4-node quadrilateral membrane, reduced integration, hourglass control) was used in ABAQUS with mesh size 1-20 resulting in 4341 nodes and 4270 elements for the whole domain. Membrane elements are surface elements that transmit in-plane forces only

(no moments) and have no bending stiffness. Therefore, out-of-plane deformation can lead to instabilities in a static analysis and a dynamic explicit step is applied to solve problems in this paper.

B. VERIFICATION OF THE ABAQUS MODEL
To check the accuracy of the ABAQUS model, a comparison of results between known analytical solution [10] and numerical simulation was carried out, in which a numerical example of isotropic membrane was used. The solution from membrane equation in this paper was also embed in the comparison. Material parameters for the membrane were taken as $E = 300MPa$, $v = 0.3$. A concentrated force of 7.85N was applied on the center of the membrane, during which

TABLE 3. The parameters during calculations with the change of Poisson's ratio.

k	$F(N)$	v_r	v_t	$E_r(MPa)$	$E_t(MPa)$	$Z\big|_{x=0}$	$dZ/dx\big|_{x=0}$	Δ
0.67	0.7854	0.3	0.2	300	200	0.3031856	181.9113	1.1e-4
0.67	0.7854	0.15	0.1	300	200	0.324484	178.4664	2.8e-5
0.67	0.7854	0.03	0.02	300	200	0.344687	175.7903	8.4e-4
0.03	0.7854	0.3	0.01	300	10	10.12979	5115.549	3.2e-4
0.03	0.7854	0.15	0.005	300	10	10.21519	5133.137	6.1e-4
0.03	0.7854	0.03	0.001	300	10	10.28810	5149.194	6.3e-4

the uniform pressure is about 0.1MPa. It is noteworthy that in order to overcome the central mesh distortion, a circular local uniform pressure with $r = R/100 = 5mm$ was used to approximate a concentrated force. It is shown that in Fig. 4, the curves obtained by membrane equation and numerical method agree well, that is to say, the ABAQUS model can work well.

IV. NUMERICAL SIMULATION USING ABAQUS

In this part, a comparison between membrane equation and numerical simulations was carried out to identify the effects of Poisson's ratio, elastic modules and thickness on load-deflection response for orthotropic membrane.

A. EFFECT OF k ON THE LOAD-DEFLECTION CURVES

MATLAB is a computer program that provides the user with a convenient environment for performing many types of calculations. One of the most popular codes in MATLAB used to solve differential equation is ODE45, which is mainly used for solving engineering applications [29]. Therefore, ODE45 was used to solve the membrane equation in this paper.

During the process to solve the membrane equation, the key factor is to determine the initial value of differential equation from Eq. (15). With the help of substituting Eq. (8) and (13) into Eq. (6) to eliminate xS_{r1} and xS_{r2}, we can obtain from Eq. (15)

$$\left. \begin{array}{l} 2\dfrac{dZ_1}{dx}\bigg|_{x=0} - \dfrac{(1+kv_r)Z_1}{x}\bigg|_{x=0} = 0 \\[4mm] 2\dfrac{dZ_1}{dx}\bigg|_{x=1} - \dfrac{(1+kv_r)Z_1}{x}\bigg|_{x=1} = 0 \end{array} \right\} \quad (16a, b)$$

When solving membrane equations, the trial and error method is used to find the initial values that meet the Eq. (15). Introduce a variable to monitor calculation error Δ.

$$\Delta = \left(2\dfrac{dZ_1}{dx}\bigg|_{x=0} - \dfrac{(1+kv_r)Z_1}{x}\bigg|_{x=0} \right)$$
$$+ \left(2\dfrac{dZ_1}{dx}\bigg|_{x=1} - \dfrac{(1+kv_r)Z_1}{x}\bigg|_{x=1} \right) \quad (17)$$
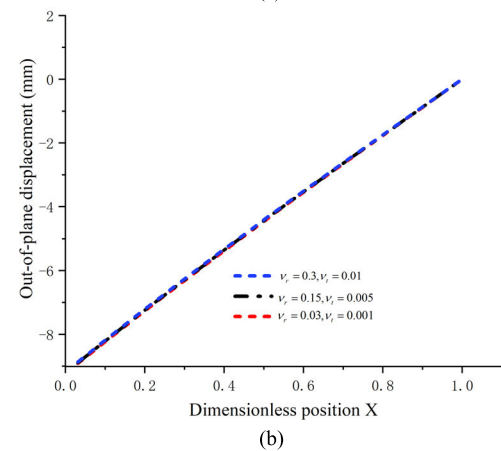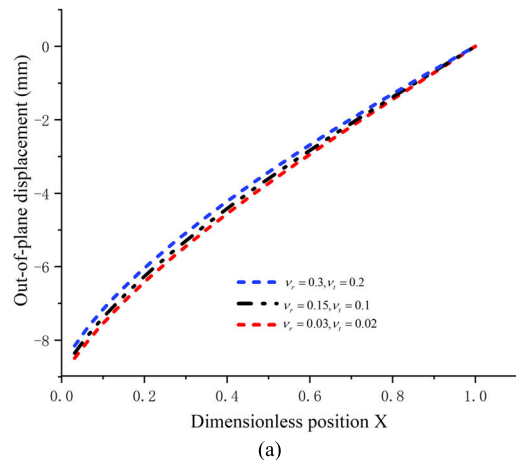

(a)

(b)

FIGURE 9. (a) Effect of Poisson's ratio on load-deflection behavior when k = 0.67. (b) Effect of Poisson's ratio on load-deflection behavior when k = 0.001.

Table 1 shows the parameters during the calculation with the change of k.

Fig. 5 shows the load-deflection curves as the value of k increases. Generally, radial Young's modulus E_r is larger than circumferential Young's modulus E_t in existing orthotropic membrane [30]; therefore, we make k not be over 1 due to Eq. (13) in this paper. As we can see, when subjected to a constant force, firstly, the load-deflection curve gradually
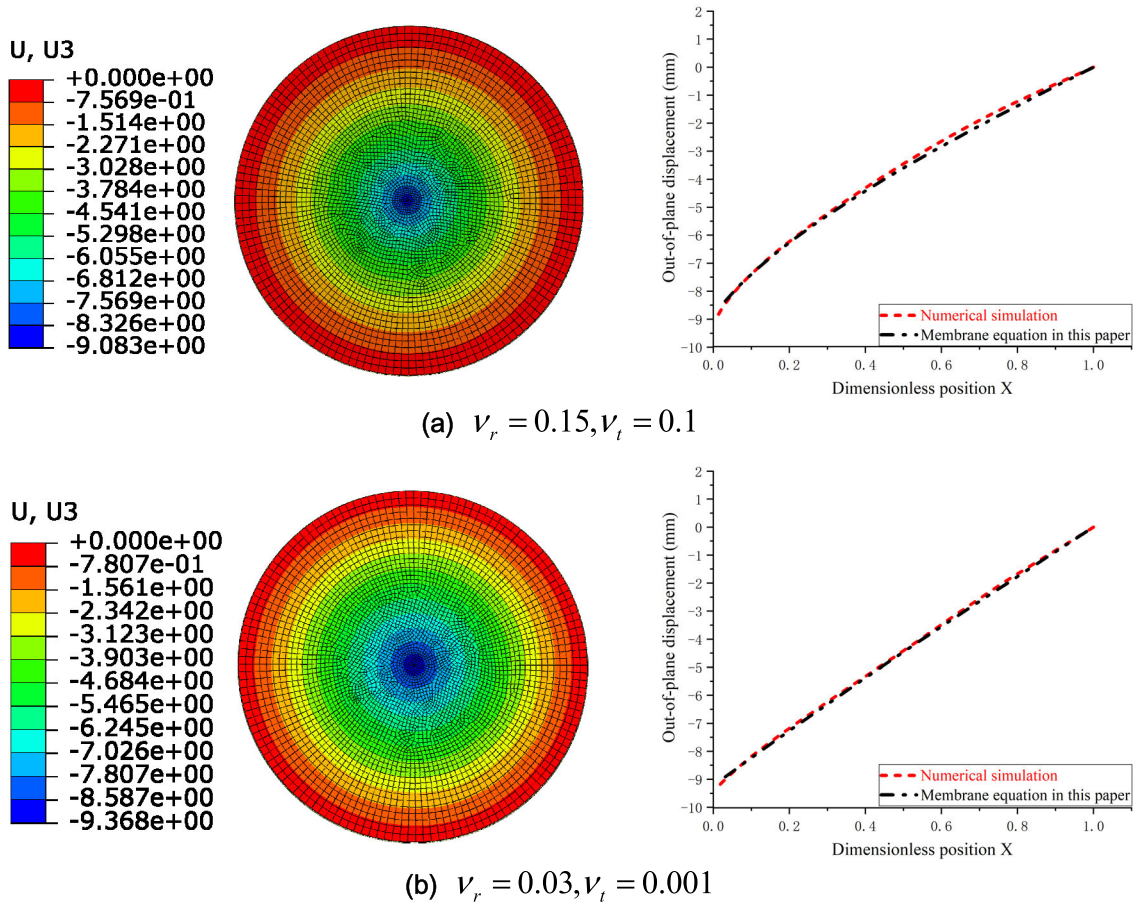
(a) $v_r = 0.15, v_t = 0.1$

(b) $v_r = 0.03, v_t = 0.001$

FIGURE 10. Comparison of load-deflection curves resulted from membrane equations and ABAQUS model.

TABLE 4. The parameters during calculations with the change of thickness *h*.

h	$F(N)$	v_r	v_t	$E_r(MPa)$	$E_t(MPa)$	$Z\big|_{x=0}$	$dZ/dx\big|_{x=0}$	Δ
1	0.7854	0.3	0.2	300	200	0.3031856	181.9113	1.1e-4
0.50	0.7854	0.3	0.2	300	200	1.9251082	1155.064	1.1e-4
0.20	0.7854	0.3	0.2	300	200	22.162997	13297.79	4.4e-4
0.10	0.7854	0.3	0.2	300	200	140.72627	84435.75	8.9e-5
0.05	0.7854	0.3	0.2	300	200	893.55609	536133.6	9.2e-4

approaches a straight line and the absolute value of the curvature approaches zero as *k* decreases. The process of change is not linear and from the time when $k = 0.03$, the change became apparent. Compared with an isotropic membrane, that is to say, we can control the shape of a membrane after deformation by changing the value of *k*. However, even the value of *k* is very close to zero, the sign of curves' curvature will not alter.

Second, the deflection of curves gradually increases when the value of *k* starts to change; however, the increase is not apparent. We can see from Fig. 2 that the decrease

of Poisson's ratio can result in the increased deflection in isotropic membranes. Therefore, the increased deflection here for orthotropic membranes maybe result from the combined action of Poisson's ration and circumferential Young's modulus.

For the finite-element approach, Fig. 6 shows the comparison of load-deflection curves between membrane equation and the numerical method. In these cases, the circular membrane has a constant thickness $h = 1mm$, radius $R = 500mm$. Different values of Radial Poisson's ratio v_r, circumferential Poisson's ratio v_t, *k* used here can be obtained from Table 1.

As shown in Fig. 6, the load-deflection curves between membrane equation and numerical simulations in ABAQUS agree well except for the area near circular membrane center. This is due to the introduction of a circular local uniform pressure on the membrane center which substitutes the concentrated force.

B. EFFECT OF ELASTIC MODULUS ON THE LOAD-DEFLECTION CURVES

Fig. 7(a) shows the comparison of load-deflection curves as elastic modulus of circular membranes decrease. From Fig.7(a), it can be seen that Poisson's ratios are kept unchanged; therefore, the value of k keeps constant. Table 2 depicts the parameters during the calculation with the change of elastic modulus.

As one can see from Fig. 7(a), the deflection of load-deflection curves increases apparently as elastic modulus decreases; however, the shape of a membrane after deformation seems unchanged, even the deflection increases to *82mm*. The role of elastic modulus in orthotropic membrane is similar to that of Poisson's ratio in isotropic membrane. The changing elastic modules, without the change of k, mainly influence the deflection of curves. Fig. 7(b) shows the deflection at the central point of circular membranes as the elastic modulus increase. The deflection decreases intensely in the low-elastic-modules material parameters and then the drop becomes gentle in high-elastic-modules material parameters. Compared with Fig. 5, we can conclude that radial Young's modulus E_r, not circumferential Young's modulus E_t, is the key factor to decide the deflection of curves.
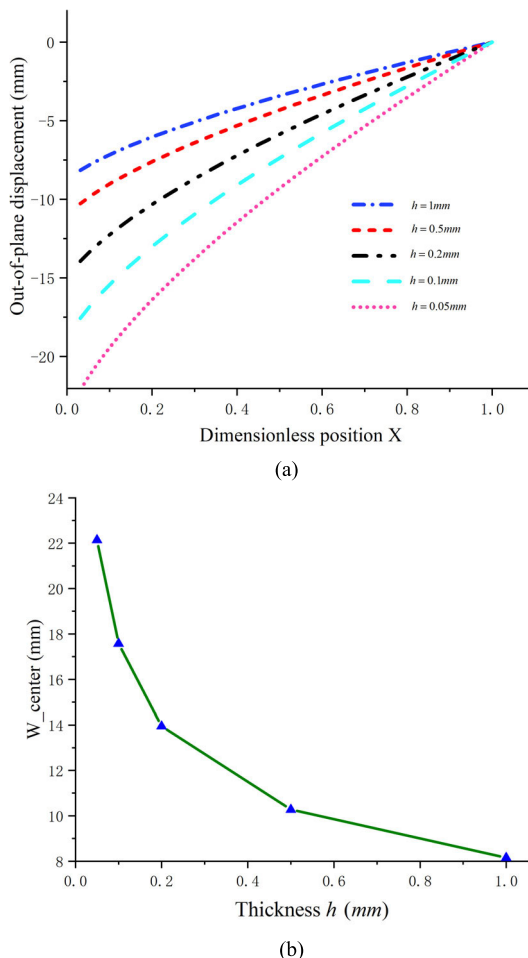
For the finite-element approach, the load-deflection curves resulted from membrane equation and the numerical method are compared in Fig. 8. In these cases, the circular membrane also has a constant thickness $h = 1mm$, radius $R = 500mm$. Radial Poisson's ratio v_r, circumferential Poisson's ratio v_t, different k value used here can be obtained from Table 2.

Fig. 8 reveals the differences of load-deflection curves from membrane equation and numerical simulations in ABAQUS. Also, the results agree poorly in the area near the center of circular membrane. In order to neglect the influence of shear modulus G, $G = 0.1MPa$ was set when simulating in ABAQUS.

C. EFFECT OF POISSON'S RATIO ON THE LOAD-DEFLECTION CURVES

Fig. 9(a) and Fig. 9(b) depict the changes of load-deflection curves as Poisson's ratio of circular membranes decreases. In Fig. 9(a) and Fig. 9(b), elastic modulus is unchanged during the whole simulation and the value of k keeps constant, respectively. Table 3 gives the parameters during the calculation.

One can observe that the deflection of load-deflection curves slightly increase as the Poisson's ratio decreases when $E_t = 200MPa$; meanwhile, the deflection nearly keeps unchanged with different Poisson' ratio when $E_t = 10MPa$. In addition, the curvature after deformation almost keeps

(a)

(b)

FIGURE 11. (a) Effect of thickness h on load-deflection behavior. (b) Effect of thickness h on the deflection of central point.

unchanged in Fig. 9(a). It is similar with the isotropic membranes in which the Poisson' ratio can have a slight effect on the deflection. Overall, only by adjusting the Poisson's ratio will not the load-deflection curves obtain significant change if the value of k almost keeps constant.

As for the results from ABAQUS, load-deflection results from membrane equation and the numerical method are compared in Fig. 10. The circular membrane has a constant thickness $h = 1mm$, radius $R = 500mm$. Other material parameters used here are given in Table 3.

From Fig. 10, one can obtain the differences between load-deflection results from membrane equation and the ones from numerical simulations. The results have nice overlap in the area near the central point of circular membrane; meanwhile, it behaves well on the rest of the curve.

D. EFFECT OF THICKNESS h ON THE LOAD-DEFLECTION CURVES

The influence of thickness h on the load-deflection behavior are compared in Fig. 11(a) and the Poisson's ratio and elastic modulus are kept constant. The parameters during the calculation with the change of thickness h can be found in Table 4.
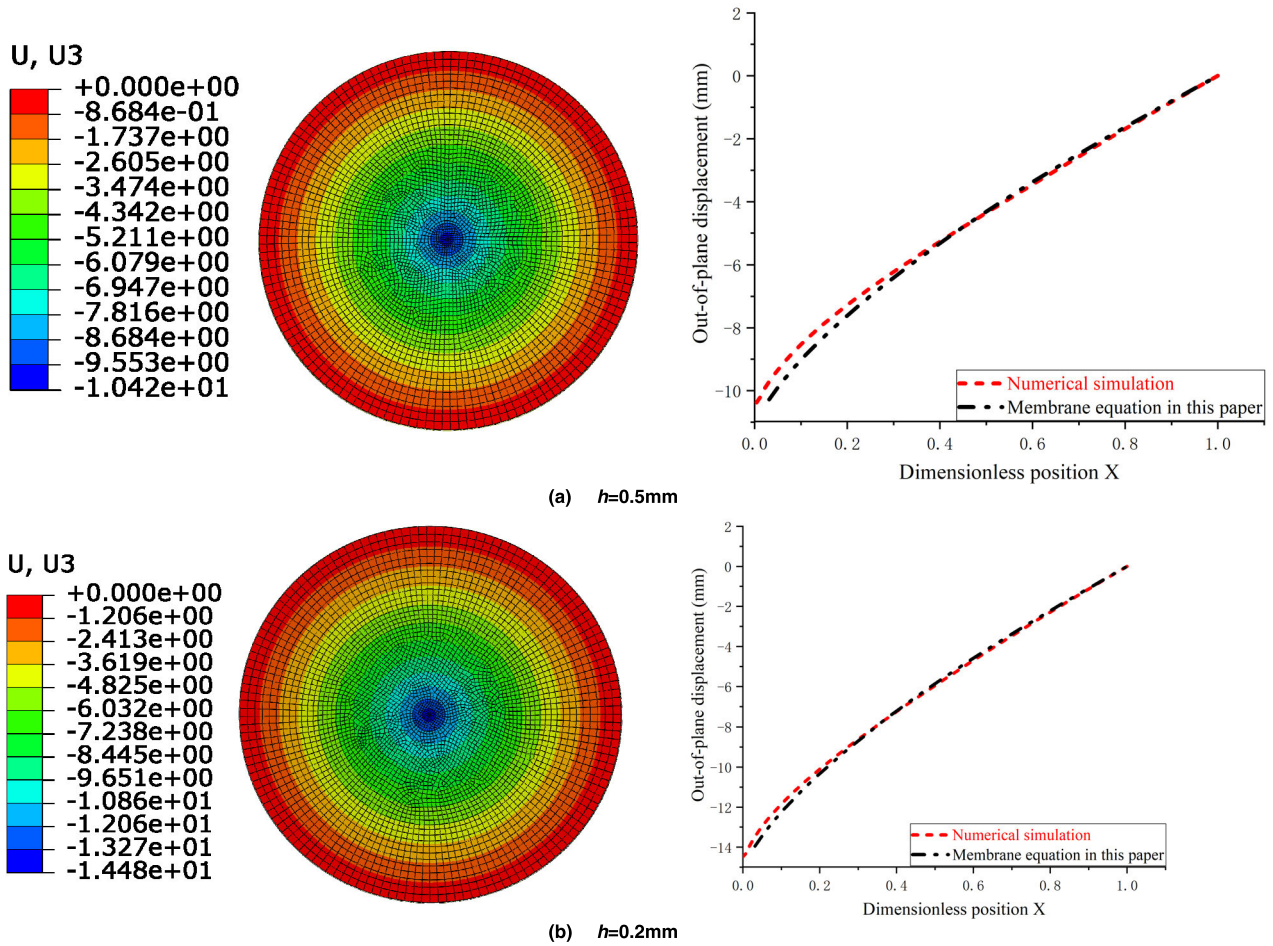
(a)   *h*=0.5mm

(b)   *h*=0.2mm

FIGURE 12. Comparison of load-deflection curves resulted from membrane equations and ABAQUS model.

Shown as Fig. 11(a), compared to elastic modules, the thickness *h* plays the similar role about the effect on the deformation of circular membrane. The decrease of thickness results in the increase of deflection; however, it has little effect on the shape of a membrane after deformation. It can be understood easily because we can see that both elastic modulus and thickness *h* mainly influence the parameter *P* from Eq. (8). The deflection at the central point of circular membranes with respect to increasing thickness are summarized in Fig. 11(b). it is obvious that the rate of deflection's decline gradually becomes gentle as thickness increases.

ABAQUS applies the similar parameters with those in above sections except the thickness. Other materials parameters can be obtained in Table 4. It can be observed in Fig. 12. that the load-deflection curves from membrane equation and ABAQUS simulation agree well in overall; however, apparent differences in the area near the center of membrane can still be seen.

V. CONCLUSIONS
In this paper, the deformation of circular orthotropic membranes subjected to a concentrated force is investigated.

Based on the work of Sun [10], we have obtained the orthotropic membrane equation and gotten the numerical solution using MATLAB. The results show that the value of *k* from Eq. (13) is the most influential parameter on the load-deflection behavior. The load-deflection curve gradually approaches a straight line when *k* is close to zero. Only change in elastic modulus and Poisson's ratio, with *k* constant, mainly influence the deflection of curves, instead of the shape of curves. The effect of thickness *h* on the load-deflection curve was also studied. The results show that the decrease of thickness *h* will result in the increase of deflection; however, it almost does not influence the shape of a membrane.

Besides, some numerical simulations by ABAQUS are conducted, which are compared with the solution from orthotropic membrane equation. All the curves, including different elastic modulus, Poisson's ratio and thickness agree well except the area near the center of membranes. The results show that the orthotropic membrane equation in this paper gives a good estimation of load-deflection behavior and can be accepted as a useful estimation of load-deflection curves for thin membrane.

REFERENCES

[1] M. Zhao, W. Zheng, and C. Fan, "Mechanics of shaft-loaded blister test for thin film suspended on compliant substrate," *Int. J. Solids Struct.*, vol. 47, nos. 18–19, pp. 2525–2532, Sep. 2010.

[2] S. Chucheepsakul, S. Kaewunruen, and A. Suwanarat, "Large deflection analysis of orthotropic, elliptic membranes," *Structural Eng. Mech.*, vol. 31, no. 6, pp. 625–638, Apr. 2009.

[3] A. Arjun and K.-T. Wan, "Derivation of the strain energy release rate g from first principles for the pressurized blister test," *Int. J. Adhes. Adhesives*, vol. 25, no. 1, pp. 13–18, Feb. 2005.

[4] Y. Tang, T. Li, and X. Ma, "Pillow distortion analysis for a space mesh reflector antenna," *AIAA J.*, vol. 55, no. 9, pp. 3206–3213, Sep. 2017.

[5] L. Datashvili, H. Baier, J. Schimitschek, M. Lang, and M. Huber, "High precision large deployable space reflector based on pillow-effect-free technology," in *Proc. 48th AIAA/ASME/ASCE/AHS/ASC Struct., Struct. Dyn., Mater. Conf.*, Apr. 2007, p. 2186.

[6] L. Wang and L. Dong-Xu, "Simple technique for form-finding and tension determining of cable-network antenna reflectors," *J. Spacecraft Rockets*, vol. 50, no. 2, pp. 479–481, Mar. 2013.

[7] H. Hencky, "Über den spannungszustand in kreisrunden platten mit verschwindender biegungssteifigkeit," *Zeitschrift Fur Math. und Physik.*, vol. 63, pp. 311–317, 1915.

[8] W. Z. Chien, "Asymptotic behavior of a thin clamped circular plate under uniform normal pressure at very large deflection," *Sci. Rep. Nat. Tsinghua Univ.*, vol. 5, no. 1, pp. 193–208, 1948.

[9] S. A. Alekseev, "Elastic circular membranes under the uniformly distributed loads," (in Russian), *Eng. Corpus.*, vol. 14, pp. 196–198, 1953.

[10] J.-Y. Sun, J.-L. Hu, X.-T. He, and Z.-L. Zheng, "A theoretical study of a clamped punch-loaded blister configuration: The quantitative relation of load and deflection," *Int. J. Mech. Sci.*, vol. 52, no. 7, pp. 928–936, Jul. 2010.

[11] K.-T. Wan, S. Guo, and D. A. Dillard, "A theoretical and numerical study of a thin clamped circular film under an external load in the presence of a tensile residual stress," *Thin Solid Films*, vol. 425, nos. 1–2, pp. 150–162, Feb. 2003.

[12] B.-F. Ju, Y. Ju, M. Saka, K.-K. Liu, and K.-T. Wan, "A systematic method for characterizing the elastic properties and adhesion of a thin polymer membrane," *Int. J. Mech. Sci.*, vol. 47, no. 3, pp. 319–332, Mar. 2005.

[13] T.-C. Lim, "Large deflection of circular auxetic membranes under uniform load," *J. Eng. Mater. Technol.*, vol. 138, no. 4, Oct. 2016, Art. no. 041011.

[14] J. Aw, H. Zhao, A. Norbury, L. Li, G. Rothwell, and J. Ren, "Effects of Poissonš ratio on the deformation of thin membrane structures under indentation," *Phys. Status Solidi (B)*, vol. 252, no. 7, pp. 1526–1532, 2015.

[15] Y. B. Fu and R. W. Ogden, Eds., *Nonlinear Elasticity-Theory and Applications* (London Mathematical Society, Lecture Notes Series 283). Cambridge, U.K.: Cambridge Univ. Press, 2001.

[16] A. P. S. Selvadurai, "Deflections of a rubber membrane," *J. Mech. Phys. Solids*, vol. 54, no. 6, pp. 1093–1119, Jun. 2006.

[17] R. Ansari, R. Hassani, M. F. Oskouie, and H. Rouhi, "Large deformation analysis in the context of 3D compressible nonlinear elasticity using the VDQ method," *Eng. Comput.*, pp. 1–13, Mar. 2020.

[18] M. F. Oskouie, M. K. Hassanzadeh-Aghdam, and R. Ansari, "A new numerical approach for low velocity impact response of multiscale-reinforced nanocomposite plates," *Eng. Comput.*, pp. 1–18, Aug. 2019.

[19] D. Liprandi, F. Bosia, and N. M. Pugno, "A theoretical-numerical model for the peeling of elastic membranes," *J. Mech. Phys. Solids*, vol. 136, Mar. 2020, Art. no. 103733.

[20] Y. Lu, H. Yue, Z. Deng, and H. Tzou, "Distributed microscopic actuation analysis of deformable plate membrane mirrors," *Mech. Syst. Signal Process.*, vol. 100, pp. 57–84, Feb. 2018.

[21] Y.-F. Lu, H.-H. Yue, Z.-Q. Deng, and H.-S. Tzou, "Adaptive shape control for thermal deformation of membrane mirror with in-plane PVDF actuators," *Chin. J. Mech. Eng.*, vol. 31, no. 1, p. 9, Dec. 2018.

[22] Y. Lu, Q. Shao, M. Amabili, H. Yue, and H. Guo, "Nonlinear vibration control effects of membrane structures with in-plane PVDF actuators: A parametric study," *Int. J. Non-Linear Mech.*, vol. 122, Jun. 2020, Art. no. 103466.

[23] D. Li, Z. Zheng, Y. Tian, J. Sun, X. He, and Y. Lu, "Stochastic nonlinear vibration and reliability of orthotropic membrane structure under impact load," *Thin-Walled Struct.*, vol. 119, pp. 247–255, Oct. 2017.

[24] N. Banichuk, J. Jeronen, M. Kurki, P. Neittaanmäki, T. Saksa, and T. Tuovinen, "On the limit velocity and buckling phenomena of axially moving orthotropic membranes and plates," *Int. J. Solids Struct.*, vol. 48, no. 13, pp. 2015–2025, Jun. 2011.

[25] J. G. Valdés, J. Miquel, and E. Oñate, "Nonlinear finite element analysis of orthotropic and prestressed membrane structures," *Finite Elements Anal. Des.*, vol. 45, nos. 6–7, pp. 395–405, May 2009.

[26] K. E. Evans and K. L. Alderson, "Auxetic materials: The positive side of being negative," *Eng. Sci. Edu. J.*, vol. 9, no. 4, pp. 148–154, Aug. 2000.

[27] Q. Huang, Z. Kuang, H. Hu, and M. Potier-Ferry, "Multiscale analysis of membrane instability by using the arlequin method," *Int. J. Solids Struct.*, vol. 162, pp. 60–75, May 2019.

[28] C. Zhang, L. Fan, and Y. Tan, "Sequential limit analysis for clamped circular membranes involving large deformation subjected to pressure load," *Int. J. Mech. Sci.*, vol. 155, pp. 440–449, May 2019.

[29] W. K. Ahmed, "Advantages and disadvantages of using MATLAB/ODE45 for solving differential equations in engineering applications," *Int. J. Eng.*, vol. 7, no. 1, pp. 25–31, 2013.

[30] H. Luo, C. Dai, R. Z. Gan, and H. Lu, "Measurement of Young's modulus of human tympanic membrane at high strain rates," *J. Biomech. Eng.*, vol. 131, no. 6, Jun. 2009.

PENGFEI HUANG was born in 1994. He received the B.S. degree from Northwestern Polytechnical University, China, in 2015, and the M.S. degree from Beihang University, China, in 2018. He is currently pursuing the Ph.D. degree with the China Academy of Space Technology (Xi'an). His research interests include structures of large deployable antenna and mechanics of membrane.

YANPING SONG was born in 1963. He received the B.S. degree from the Beijing Institute of Technology, Beijing, China, in 1984, and the M.S. degree from Xidian University, in 1987. He is currently a Research Fellow with the China Academy of Space Technology (Xi'an). His research interests include structures of composites and large deployable antenna.

QI LI was born in 1992. He received the B.S. and Ph.D. degrees from Northwestern Polytechnical University, Xi'an, China, in 2015 and 2020, respectively. His research interest includes satellite navigation control.

XIAOQI LIU was born in 1992. She received the B.S. degree from Liaoning University, Shenyang, China, in 2014, and the M.S. degree from Aviation Industry Corporation of China, in 2018. She is currently an Engineer with the China Academy of Space Technology (Xi'an).

YUQING FENG was born in 1997. She received the B.S. degree from the Nanjing University of Aeronautics and Astronautics, Nanjing, China, in 2018. She is currently pursuing the master's degree with the China Academy of Space Technology (Xi'an), Xi'an, China. Her research interests include structures of large deployable antenna and structural vibration.

● ● ●